Single-channel SCAM Identifies Pore-lining Residues in the First Extracellular Loop and First Transmembrane Domains of Cx46 Hemichannels

J. Kronengold,[1] E.B. Trexler,[2] F.F. Bukauskas,[1] T.A. Bargiello,[1] and V.K. Verselis[1]

[1]Department of Neuroscience, Albert Einstein College of Medicine, New York, NY 10461
[2]Department of Ophthalmology and Visual Science, University of Texas-Houston Medical School, Houston, TX 77030

ABSTRACT Gap junction (GJ) channels provide an important pathway for direct intercellular transmission of signaling molecules. Previously we showed that fixed negative charges in the first extracellular loop domain (E1) strongly influence charge selectivity, conductance, and rectification of channels and hemichannels formed of Cx46. Here, using excised patches containing Cx46 hemichannels, we applied the substituted cysteine accessibility method (SCAM) at the single channel level to residues in E1 to determine if they are pore-lining. We demonstrate residues D51, G46, and E43 at the amino end of E1 are accessible to modification in open hemichannels to positively and negatively charged methanethiosulfonate (MTS) reagents added to cytoplasmic or extracellular sides. Positional effects of modification along the length of the pore and opposing effects of oppositely charged modifying reagents on hemichannel conductance and rectification are consistent with placement in the channel pore and indicate a dominant electrostatic influence of the side chains of accessible residues on ion fluxes. Hemichannels modified by MTS-EA$^+$, MTS-ET$^+$, or MTS-ES$^-$ were refractory to further modification and effects of substitutions with positively charged residues that electrostatically mimicked those caused by modification with the positively charged MTS reagents were similar, indicating all six subunits were likely modified. The large reductions in conductance caused by MTS-ET$^+$ were visible as stepwise reductions in single-channel current, indicative of reactions occurring at individual subunits. Extension of single-channel SCAM using MTS-ET$^+$ into the first transmembrane domain, TM1, revealed continued accessibility at the extracellular end at A39 and L35. The topologically complementary region in TM3 showed no evidence of reactivity. Structural models show GJ channels in the extracellular gap to have continuous inner and outer walls of protein. If representative of open channels and hemichannels, these data indicate E1 as constituting a significant portion of this inner, pore-forming wall, and TM1 contributing as pore-lining in the extracellular portion of transmembrane span.

KEY WORDS: gap junctions • connexin • rectification • conductance • cysteine scanning

INTRODUCTION

Gap junction (GJ) channels, formed by the gene family of connexins, provide an important pathway for direct intercellular signaling in many tissues. To date there are 19 connexin genes identified in rodents and 20 in humans, with tissue- and cell-specific, but overlapping patterns of expression (Willecke et al., 2002). Unitary conductances and charge selectivities differ sufficiently among connexin channels (Veenstra et al., 1995; Harris, 2001; Valiunas et al., 2002), suggesting the expression of certain connexins may reflect a requirement for transmission or restriction of specific signaling molecules. Mutations in connexins have been shown to be responsible for hereditary human diseases including the X-linked form of Charcot-Marie-Tooth (CMTX) demyelinating diseases (Bergoffen et al., 1993; Ionasescu et al., 1994), nonsyndromic sensorineural deafness (Kelsell et al., 1997), erythrokeratodermia (Richard et

al., 1998), and congenital cataractogenesis (Shiels et al., 1998; Mackay et al., 1999).

Formed by the docking of two hemichannels, one from each of two closely apposed cells, a GJ or cell–cell channel constitutes a long pore that traverses the membranes of two apposed cells and the gap between them. A hemichannel, which represents a typical ion channel configuration spanning a single membrane, is composed of a hexamer of connexin subunits. The accepted membrane topology of a connexin subunit has four transmembrane domains with amino and carboxy termini located intracellularly (Paul, 1986; Hertzberg et al., 1988; Bennett et al., 1991). The two loops, E1 and E2, that connect the transmembrane domains on the extracellular side almost certainly mediate the docking of two hemichannels, but it is now evident that unapposed or undocked hemichannels can also function in the plasma membrane outside regions of cell–cell contact (Paul et al., 1991; Ebihara and Steiner,

Address correspondence to Vytas K. Verselis, Department of Neuroscience, Albert Einstein College of Medicine, 1300 Morris Park Avenue, New York, NY 10461. Fax: (718) 430-8944; email: verselis@aecom.yu.edu

1993; Harris, 2001). A gating mechanism sensitive to membrane voltage and extracellular divalent cations, distinct from the well-known transjunctional voltage-gating mechanism described in cell–cell channels, has been proposed to mediate opening of unapposed hemichannels (Trexler et al., 1996; Oh et al., 2000; Verselis and Bukauskas, 2002). Unlike the E1 and E2 domains of docked hemichannels, which interact to establish a cell–cell channel pore insulated from the extracellular gap, the E1 and E2 domains of unapposed hemichannels remain free to form the external vestibule of the hemichannel pore. Although some differences in structure and properties may occur between docked and undocked hemichannels, conserved gating and permeability characteristics of cell–cell channels and corresponding unapposed hemichannels suggest the two structures are minimally different (Ebihara et al., 1995; Trexler et al., 1996, 1999; Oh et al., 2000; Verselis et al., 2000; Beahm and Hall, 2002).

Differences in permeability characteristics of GJ channels and hemichannels are likely important in conferring connexin-specific function and suggest there is some variation in pore-ling residues. Substituted cysteine accessibility mutagenesis studies (SCAM; Karlin and Akabas, 1998) using a large maleimide thiol reagent, maliemidobutyryl biocytin (MBB, MW 537), applied to Cx46 and chimeric Cx32*43E1 hemichannels have reported sparse accessibility in TM1 and TM3 (Zhou et al., 1997). A SCAM study applied to Cx32 cell–cell channels using MBB and a dual-oocyte perfusion technique reported TM3 to be pore lining with six reactive residues showing a periodicity consistent with a tilted α-helix (Skerrett et al., 2002).

Using domain exchange and solutions of varying ionic strength, we showed that the E1 domain of Cx46 contributes fixed negative charges that strongly influence charge selectivity and open hemichannel rectification, suggesting residues in E1 contribute to the pore (Trexler et al., 2000). Here we used Cx46 hemichannels to examine solvent accessibility of Cys substituted amino acids in E1 and establish their residence in the pore. To distinguish between gating and conductance effects and also to distinguish between residues remote from the pore that may affect open channel properties indirectly, we monitored effects of modification at the single-channel level using excised patches and application of modifying reagents from either side of the membrane. Furthermore, we took advantage of the generally large size of connexin channels and their ability to pass both cations and anions to examine the effects of modification by positively and negatively charged methanethiosulfonate (MTS) reagents, with the expectation that pore-lining residues modified to positive or negative charge should produce different effects on ion fluxes through open channels qualitatively

consistent with the opposite electrostatic properties imposed. Based on sidedness of accessibility in open hemichannels and effects on open hemichannel properties, we demonstrate residues in E1, near the E1/TM1 border, to be pore-lining. Two of the identified residues in E1 are negatively charged and likely constitute the locus of fixed negative charge previously indicated by domain substitution. Continued accessibility of residues in TM1 indicates that the pore continues from E1 to TM1 as it enters the transmembrane span.

MATERIALS AND METHODS

Construction of Cys Substitutions in E1 of Cx46

The rat Cx46 coding sequence cloned into EcoRI-HindIII of pGem7zf(+) was used as a template to construct all mutants. To make the E1 (Glu42–Asp51) cysteine, point mutations and double mutants we first introduced NarI and PstI sites by silent mutagenesis to create unique cloning sites(rCx46-M1E1-np-wt). We then substituted corresponding PCR generated fragments containing the various mutations. Specifically, NarI and PmlI were used for E42C, whereas PstI was used for E43C through D51C; the latter required additional screens for orientation using BsaAI before sequencing. The TM1 mutants were made using the rCx46-M1E1-np-wt construct with NarI and PmlI as cloning sites for A41C and A40C and EcoRI and PstI for the remaining sites. To make the TM3 mutants, we first introduced SalI and MscI sites by silent mutagenesis into the full-length rCx46wt. A SalI/BstXI 330bp fragment was cloned into pGem to make an M3mut cassette. Mutants were generated on this cassette using PshAI-PstI (F157C-T163C), MscI-PmlI (L164C-I170C), and PstI-PmlI (A171C-F175C). Cysteine mutants were then backcloned into rCx46wt. All constructs were sequenced over the restriction sites used for cloning.

Expression of Hemichannels in Xenopus Oocytes

mRNA was prepared from appropriately linearized plasmid DNA with the mMessage mMachine T7 RNA kit from Ambion according to the manufacturer's protocol. The mRNA was purified using QIAquick PCR purification columns from QIAGEN. mRNA bound to the column was eluted with 30–40 μl of an aqueous solution of DNA antisense to the endogenous XenCx38 (8 pmole/ml). We used the phosphorothioate antisense oligo 5′-GCT TTA GTA ATT CCC ATC CTG CCA TGT TTC-3′, which is complementary to XenCx38 commencing at NT −5 with respect to the ATG initiation codon. For experiments in which wtCx46 and Cx46(G46C) were coexpressed, cRNA concentrations were determined spectrophotometrically and mixed in appropriate ratios for injection. Preparation of *Xenopus* oocytes has been described previously (Rubin et al., 1992a,b). Each oocyte was injected with 50–100 nl of the mRNA/antisense solution. Injected oocytes were kept at 18°C in a standard solution containing (in mM) 88 NaCl, 1 KCl, 2 MgCl$_2$, 1.8 CaCl$_2$, 5 glucose, 5 HEPES, 5 PIPES, 5 pyruvate pH 7.6.

Preparation of Reagents and Recording Solutions

In macroscopic recordings of hemichannel currents, *Xenopus* oocytes were bathed in a modified ND96 solution containing (in mM) 88 NaCl, 1 KCl, 2 MgCl$_2$, 1.8 CaCl$_2$, 5 glucose, 5 HEPES, pH 7.6. Both current-passing and voltage-recording pipettes were filled with 2M KCl. For patch clamp recordings of hemichannel currents, *Xenopus* oocytes were manually devitellinized in a hypertonic solution consisting of (in mM) 220 Na aspartate, 10 KCl, 2

MgCl$_2$, 10 HEPES and then placed in the ND96 solution with no added Ca^{2+}. Internal patch pipette solutions (IPS) used for recording hemichannels consisted of (in mM) 140 KCl, 5 EGTA, 1 CaCl$_2$, 1 MgCl$_2$, 5 HEPES and pH was adjusted to 7.6 with KOH.

MTS reagents, 2-aminoethylmethane thiosulfonate (MTS-EA$^+$), 2-trimethylammonioethyl-methane thiosulfonate (MTS-ET$^+$), and 2-sulfonatoethylmethane thiosulfonate (MTS-ES$^-$) were purchased from Anatrace. Aliquots of dry powder were prepared and stored in microcentrifuge tubes at $-20°$C. Prior to each experiment an aliquot was dissolved in distilled water, chilled on ice, to a stock concentration of 250 mM. Dilutions were made into IPS just before application to the desired final concentration (ranging from 0.25 to 5 mM). Activity of MTS reagents were periodically checked using a TNB assay (Karlin and Akabas, 1998).

Electrophysiological Recording and Analysis

Functional expression of Cys-substituted mutants was screened using two-electrode voltage clamp recordings of macroscopic currents from single *Xenopus* oocytes using a GeneClamp 500 amplifier (Axon Instruments, Inc.). Currents were digitized using pClamp 6.0 software and a Digidata 1200 interface (Axon Instruments, Inc.).

Single hemichannel currents in *Xenopus* oocytes were recorded using an Axopatch 1D amplifier (Axon Instruments, Inc.). Devitellinized oocytes were placed in an excised patch chamber (RC-28; Warner Instruments Corp.) consisting of two bath compartments separated by a dam/reservoir. Oocytes were placed in the larger bath compartment. The smaller bath compartment was connected via a 3 M agar bridge to a ground compartment containing the same IPS solution as in the bath compartments and the pipette. Both compartments were initially connected by flooding over the dam. After excision of patches containing single hemichannels, instrumentation offsets were manually corrected in the absence of an applied voltage. Excised patches were then moved across the dam/reservoir to the smaller compartment, whereupon emptying the dam/reservoir by vacuum suction separated the compartments. Hemichannel activity at a fixed voltage was recorded to establish a baseline after which the compartment was perfused with freshly prepared MTS reagent. Single hemichannel I-V curves were obtained before and after MTS application by applying 8-s voltage ramps from -70 to $+70$ mV. Unitary conductances plotted represent the slope conductances at $V_m = 0$ obtained from fitted open channel I-V relations. Open hemichannel current rectification was measured as the ratio of the currents at -70 mV and at $+70$ mV (I_{-70}/I_{+70} for inward rectification and I_{+70}/I_{-70} for outward rectification; a ratio of 1.0 indicates a linear I-V relationship).

In all patch clamp experiments with single hemichannels, the patch pipettes and bathing media consisted of IPS (see MATERIALS AND METHODS). Currents were filtered at 1 kHz and data were acquired at 10 kHz. Patch clamp data from hemichannels was acquired with AT-MIO-16X D/A boards from National Instruments using our own acquisition software.

RESULTS

Restoring E1 Residues at Positions 49 and 51 in the Cx46*32E1 Chimera Largely Restores wtCx46 Hemichannel Conductance and Rectification

Substitution of the E1 domain of Cx46 with that of Cx32 was shown to reduce unitary conductance fivefold, convert open hemichannel current rectification from inward to outward and change permeability from

cation- to anion-preferring (Trexler et al., 2000). The simplest interpretation of these results is that the E1 domain contributes to the pore and differences in sequence between Cx32 and Cx46 are responsible for the differences in open-channel properties. Fig. 1 A shows a sequence comparison of the E1 domains of Cx46,
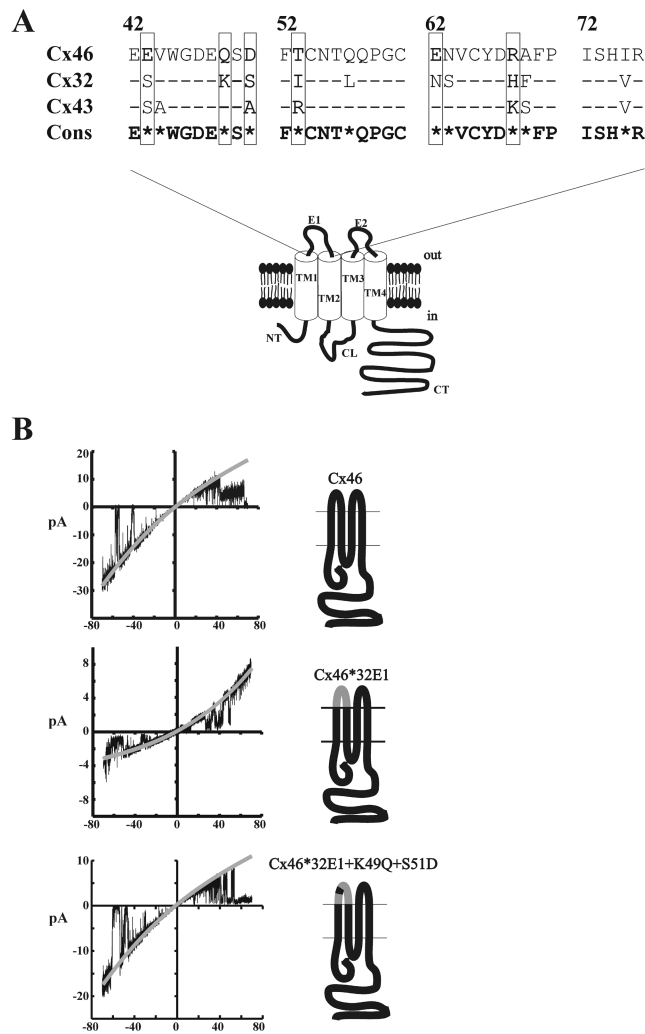
FIGURE 1. Residues in E1 of Cx46 near the TM1 border of Cx46 are important for the effects caused by the Cx46*32E1 substitution. (A) Sequence comparison of E1 domains of Cx46, Cx32, and Cx43. The accepted topology of a connexin subunit has four transmembrane (TM) domains, extracellular E1 and E2 loops, and cytoplasmic NH$_2$-terminal (NT), loop (CL), and carboxy terminal (CT) domains. E42 resides at the TM1/E1 border and R76 at the E1/TM2 border. (B) Representative recordings of Cx46, Cx46*32E1, and Cx46*32E1(K49Q + S51D) hemichannel currents in *Xenopus* oocytes obtained with 8-s voltage ramps from -70 to $+70$ mV applied to cell-attached patches containing single hemichannels. The solid gray lines represent exponential fits to the open-state current. Substitution of the E1 domain of Cx32 into Cx46 (Cx46*32E1) substantially reduced unitary conductance and converted open-channel current rectification from inward to outward. Restoring the residues at positions 49 and 51 in the Cx46*32E1 chimera back to Cx46 sequence largely restored wild-type Cx46 properties.

Cx32, and Cx43. Based on dye spread and ionic substitution studies in cell pairs, Cx46 exhibits a preference for cations, Cx32 for anions, and Cx43 no obvious preference on the basis of charge (Trexler et al., 2000). In Cx46, 5 residues with negatively charged side chains are clustered in a 10-residue stretch in E1 starting at E42 at the TM1/E1 border. In Cx32 and Cx43, two of these residues, E43 and D51, are replaced with Ser or Ala. Cx32 contains an additional positively charged Lys in place of Q49 giving Cx46 more negative charge in this region of E1 than Cx32 or Cx43. Because the combination of charges at positions 49 and 51 correlated with the selectivity characteristics of Cx46, Cx32, and Cx43, we modified the Cx46*32E1 chimera by converting residues 49 and 51 back to Cx46 sequence (Cx46*32E1(K49Q + S51D). The conductance of this channel was restored to ∼65% of wtCx46 (measured as the slope conductance at $V_m = 0$) and the open hemichannel I-V relation converted back to inwardly rectifying (Fig. 1 B). These results indicate that either or both residues at positions 49 and 51 in E1 of Cx46 are important for the effects caused by the Cx32 E1 substitution.

SCAM of E1 Residues with MTS-ET[+]

Having localized a region within E1 of Cx46 in which residues have a strong influence on single-channel conductance, open-channel current rectification, and charge selectivity, we singly replaced each position from E43 through D51 with a Cys residue to examine whether any of these residues are solvent accessible using SCAM. Of the nine substituted positions, only W45C failed to form functional hemichannels as determined by the lack of large, slowly activating outward currents at inside-positive voltages upon injection of mRNA into *Xenopus* oocytes. At the other positions, Cys substitution caused no measurable change in unitary conductance compared with wtCx46 at E43, V44, and G46 and only moderate reductions (5–15%) at, E48, Q49, S50, and D51 (Fig. 2 A). At one position, D47, unitary conductance decreased substantially (∼33%). Modest changes were also observed in open hemichannel current rectification, but all remained inwardly rectifying (Fig. 2 B).

To screen solvent accessibility, we started with the MTS derivative MTS-ET[+], which has a low membrane permeability due to its being permanently charged and a rapid reaction rate with residues at water-accessible surfaces (Karlin and Akabas, 1998). Given that residues in transmembrane segments of ion channels have been reported accessible through aqueous crevices separate from the pore (e.g., Cha and Bezanilla, 1998; Glauner et al., 1999), we constrained our accessibility studies to the single hemichannel level using the following criteria for assignment to the pore; (a) a residue must be ac-
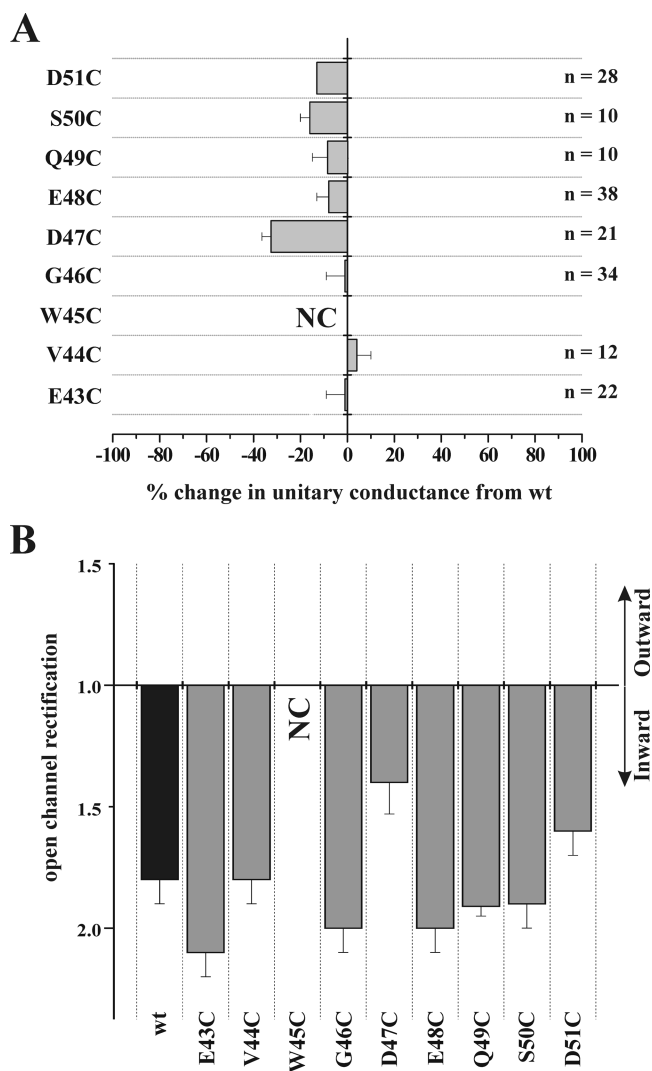
FIGURE 2. Individual Cys substitutions from E43 through D51, with the exception of W45C, form functional hemichannels. Plotted are changes in unitary conductance (A) and magnitudes of single open-hemichannel current rectification (B). The change in unitary conductance represents the mean percentage change in the slope conductance compared with wt Cx46 measured at $V_m = 0$ from fitted open channel I-V relations. Open hemichannel current rectification was measured as the ratio of the currents at −70 mV and at +70 mV (see MATERIALS AND METHODS). NC denotes nonfunctional hemichannels. Error bars represent standard deviations. For each mutant, n represents the number of separate patches examined containing single hemichannels.

cessible when the hemichannel is in the open state and (b) access must be gained in the open state with MTS reagent added from either extracellular or cytoplasmic sides of the hemichannel. Residues meeting these criteria were located at three positions, E43, G46, and D51 (Fig. 3 A). In each case, application of MTS-ET[+] from either side of an open hemichannel resulted in a substantial decrease in unitary conductance. Each of the modified hemichannels also showed reduced

MTS-ET⁺

A

D51C	n = 21
S50C	n = 12
Q49C	n = 8
E48C	n = 16
D47C	n = 14
G46C	n = 18
W45C	NC
V44C	n = 10
E43C	n = 14
wt	n = 10

% change in unitary conductance at $V_m = 0$

B

open channel rectification

Inward — Outward

wt   E43C   G46C   D51C

C   D51C

1 mM MTS-ET⁺   wash

open
closed

3 pA
10 sec

open
closed

3 pA
1 sec

D

D51C
D51C + MTS-ET⁺

I (pA)

V (mV)
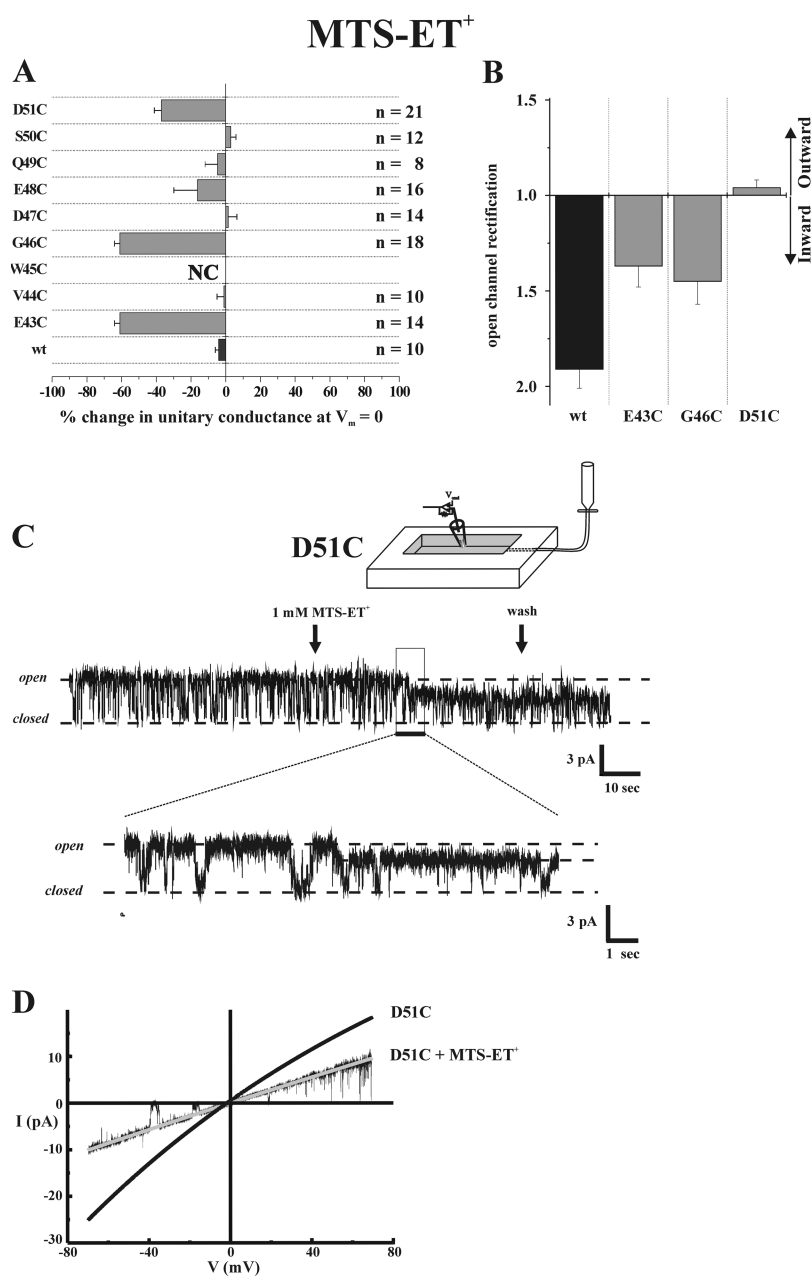
FIGURE 3. SCAM using MTS-ET⁺ shows three residues in E1 accessible to modification in single open hemichannels. (A) Plot of the percentage change in unitary conductance for each residue after application of 1.0 mM MTS-ET⁺. The change in unitary conductance represents the mean percentage change in the slope conductance relative to the corresponding Cys substituted mutant measured at $V_m = 0$ from fitted open channel I-V relations. Access from cytoplasmic and extracellular faces of the hemichannel was examined by bath-application of MTS-ET⁺ to inside-out and outside-out patches, respectively. Data from excised patches of either configuration showed no differences and were pooled together with cell-attached recordings of prereacted oocytes. Large reductions in conductance were observed at three positions: E43C, G46C, and D51C. wtCx46 hemichannel currents showed no measurable change with 1 mM MTS-ET⁺. Error bars represent standard deviations. For each mutant, n represents the number of separate patches examined containing single hemichannels. NC denotes nonfunctional hemichannels. (B) Plot of open hemichannel current rectification in wt Cx46 (black bar) and E43C, G46C, and D51C hemichannels reacted with MTS-ET⁺. The degree of inward rectification decreased in all cases, most notably at D51C in which rectification turned slightly outward. Data were obtained from the same patches as in A. (C) Example of MTS-ET⁺ modification of a single D51C hemichannel. Shown is a current record obtained from an inside-out patch containing a single D51C hemichannel. The membrane potential was held constant at 30 mV. 1 mM MTS-ET⁺ was applied to the bath (first arrow). Unitary current decreased abruptly ∼20 s after application of MTS-ET⁺ and remained stable after washout (second arrow). An expanded view is shown of the region indicated by the black bar. (D) Comparison of single open hemichannel I-V curves of the same D51C hemichannel obtained before and 2 min after application and subsequent washout of MTS-ET⁺. The prereacted open hemichannel current is represented by a solid black line obtained from an exponential fit to the data from a single ramp.

open hemichannel current rectification, particularly at D51C, where rectification between ±70 mV changed from nearly 2:1 inward to slightly outward (Fig. 3 B). These changes in open hemichannel properties remained after washout, consistent with covalent modification. Although reductions in conductance were observed at E48C, assignment to the pore is uncertain as the effects were variable in size and could not be confirmed to occur from the cytoplasmic side. Wild-type Cx46 hemichannel currents did not change with application of MTS-ET⁺ at concentrations up to 2 mM despite the presence of three cysteines in each extracellular loop; these Cys residues are conserved among all connexins and appear to form disulphide linkages important for maintaining structural integrity of the channel (Dahl et al., 1991; Foote et al., 1998). Fig. 3 C shows an example of a modification of a single D51C hemichannel using 1 mM MTS-ET⁺ applied to the cytoplasmic side of the hemichannel. Membrane potential across the patch was held constant at 30 mV to maintain a high open probability. Unitary current decreased abruptly ∼20 s after the start of application of MTS-ET⁺ to the bath and remained after washout. Comparison of the I-V curves of the same hemichannel before and 2 min after washout of MTS-ET⁺ shows the pronounced changes in open hemichannel properties (Fig. 3 D). Changes in gating were also observed, but were not examined in detail. For each Cys mutant,

A

B

C

D

FIGURE 4. SCAM using MTS-ES⁻ shows an increase in conductance and rectification at D51C. (A) Plot of the percentage change in unitary conductance for each residue after application of 5.0 mM MTS-ES⁻. For each residue, unitary conductance represents the mean percentage change in the slope conductance relative to the corresponding Cys substituted mutant measured at $V_m = 0$ from fitted open channel I-V relations. As for MTS-ET⁺, data from inside-out and outside-out patches showed no differences and were pooled together with cell-attached recordings of prereacted oocytes. Only D51C hemichannels showed a measurable change with MTS-ES⁻ and that was an increase rather than a decrease in conductance. Boxed residues are those found to be modified by MTS-ET⁺. wtCx46 hemichannel currents showed no measurable change with 5 mM MTS-ES⁻. Error bars represent standard deviations. For each mutant, n represents the number of separate patches examined containing single hemichannels. NC denotes nonfunctional hemichannels. (B and C) Examples of single hemichannel I-V relations of D51C hemichannels before and after reaction with (B) MTS-ET⁺ and (C) MTS-ES⁻. Left panels show reacted single D51C hemichannels; black lines are fits to the open hemichannel currents from single voltage ramps. Right panels show superimposed fits of the data to D51C hemichannel currents before (solid black lines) and after (solid gray lines) reaction with MTS-ET⁺ or MTS-ES⁻. Fits to wt Cx46 (dashed lines) open hemichannel currents are included for comparison. For each MTS reagent, the fitted open hemichannel currents shown before and after addition of reagent are from the same hemichannel. (D) Summary of data comparing unitary conductance (left panel) and open channel rectification of wt Cx46, unreacted D51C, and D51C reacted with MTS-ET⁺ and MTS-ES⁻. The solid horizontals lines denote mean values for conductance and rectification of wt Cx46 hemichannels. Error bars represent standard deviations. For each mutant, n represents the number of separate patches examined containing single hemichannels.
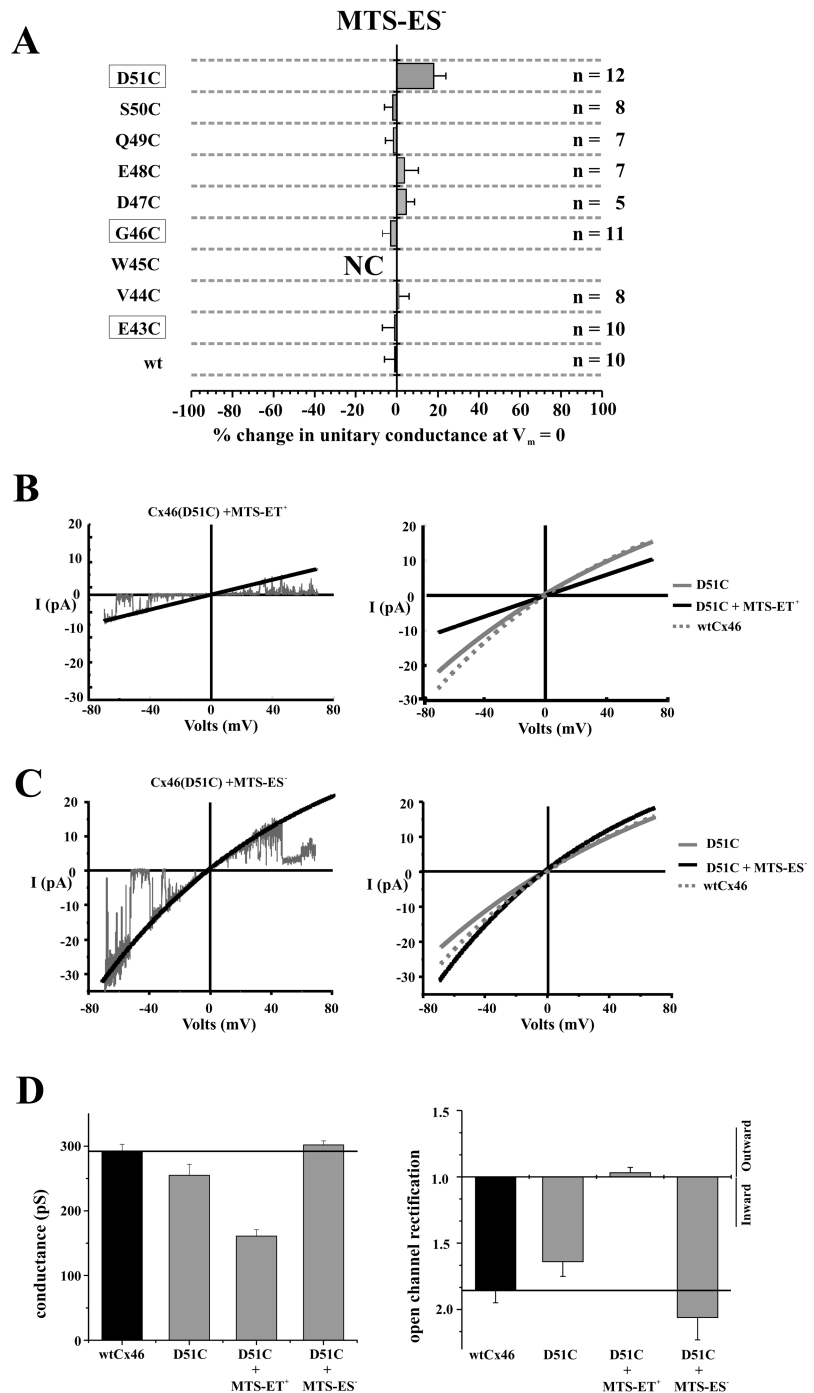
patching onto *Xenopus* oocytes treated for 10 min with MTS-ET⁺ gave the same results, indicating that the modifications were not dependent on patch configuration and were not mediated by secondary cytoplasmic factors.

MTS-ET⁺ and MTS-ES⁻ Have Opposite Effects on D51C Open Hemichannel Currents

Because GJs are large pores that can accommodate both anions and cations, we examined whether MTS-ES⁻ gained access to the same sites as MTS-ET⁺ and whether the resulting open-channel properties differed in a manner consistent with modification to a negative, rather than a positive charge. Fig. 4 A summarizes data for MTS-ES⁻. The residues that showed no effect with MTS-ET⁺ similarly showed no effect with MTS-ES⁻. Of the three residues reactive to MTS-ET⁺ (boxes) only D51C was noticeably affected by MTS-ES⁻ and that was an increase, rather than a decrease in conductance. The same results were obtained from inside-out and
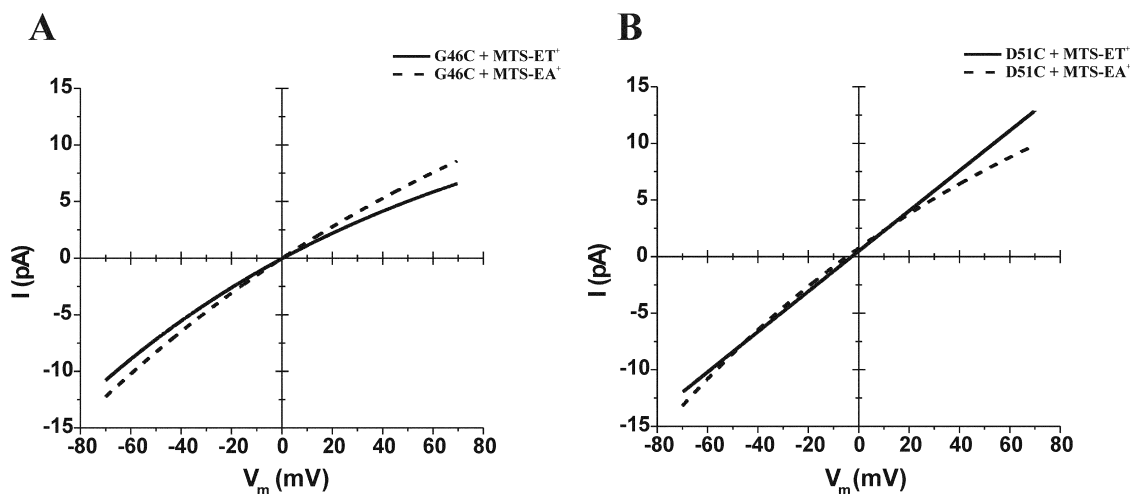
FIGURE 5. Effects of modification with MTS-EA⁺ differ modestly from that with MTS-ET⁺. Examples of I-V relations of single open G46C (A) and D51C (B) hemichannel currents after application and washout of MTS-EA⁺ (dashed lines) or MTS-ET⁺ (solid lines). The lines represent fits to the data for single voltage ramps. Mean values are illustrated in Fig. 6 B.

outside-out patches indicating the same modification occurred with reagent added to either side of the hemichannel. Superimposition of fitted open hemichannel I-V curves for wtCx46 and D51C hemichannels, reacted and unreacted, shows the modest reduction in current caused by Cys substitution alone and the large reduction caused by modification by MTS-ET⁺ (Fig. 4 B). In contrast, D51C hemichannels modified by MTS-ES⁻ showed increased unitary conductance and rectification to values slightly exceeding even those of wtCx46 (Fig. 4 C). Comparison of the effects of MTS-ET⁺ and MTS-ES⁻ on open hemichannel conductance and rectification of D51 obtained from multiple patches is summarized in Fig. 4 D.

The lack of an effect of MTS-ES⁻ on E43C and G46C open hemichannel currents could result from absence of modification due to inaccessibility or from modification with no measurable effect, i.e., a silent reaction. To distinguish between these possibilities, we examined whether MTS-ET⁺–induced modification of E43C and G46C was occluded by prior treatment with MTS-ES⁻. In both cases, MTS-ET⁺ failed to reduce conductance following a 5–10 min pretreatment with MTS-ES⁻ (unpublished data). This result indicates that modification by MTS-ES⁻ occurs at E43C and G46C, but that at these positions replacement of a Cys side chain with a negatively charged side chain has little effect on open hemichannel properties.

Effects of MTS-EA⁺ Differ Modestly from Those of MTS-ET⁺

The markedly differing effects of modification with MTS-ES⁻ and MTS-ET⁺, which place side chains of similar size, but of opposite charge, indicate that charge rather than volume is largely responsible for the observed effects of MTS reagents on open hemichannel properties. Thus, we compared the effects of MTS-ET⁺ with that of MTS-EA⁺ at two positions, G46C and D51C. Both MTS derivatives carry a positive charge, but the amine head of MTS-EA⁺ is smaller than the trimethylammonium head of MTS-ET⁺ (see Fig. 9 A). Both MTS derivatives substantially reduced hemichannel conductance. The magnitude of the effect was modestly smaller for MTS-EA⁺. Superimposition of fits to MTS-EA⁺– and MTS-ET⁺–modified open hemichannel currents show the differences in the I-V relations (Fig. 5, A and B). G46C hemichannels modified with both reagents maintained inward rectification, but open-channel currents decreased more when modified by MTS-ET⁺. For D51C, modification by MTS-EA⁺ produced hemichannels with slight inward rectification rather than the slight outward rectification characteristic of modification by MTS-ET⁺ (see also Fig. 6 B). Thus, although the electrostatic properties of the side chains conferred by MTS modification appear to be largely responsible for the observed changes in single-hemichannel conductance and rectification, side-chain volume on the order of the size difference between amine and trimethylammonium groups of MTS-EA⁺ and MTS-ET⁺, respectively, may contribute. It may be that the generally larger reduction in conductance upon MTS-ET⁺ compared with MTS-EA⁺ modification reflects increased volume and/or charge density with the same charge being placed on a bulkier group.

All Subunits Appear to be Modified by Small MTS Reagents

Considering that connexin hemichannels are homomeric hexamers, optimally there could be six conductance changes representing reactions with individual

A   **G46C**

V = +30 mV

FIGURE 6.   All six subunits in Cx46 hemichannels are likely modified by MTS-ET$^+$. (A) Example of an MTS-ET$^+$ modification of G46C. Shown is a current record obtained from an inside-out patch containing a single G46C hemichannel. The membrane potential was held constant at 30 mV and 0.25 mM MTS-ET$^+$ was applied to the bath (indicated by the bar). Unitary current decreased ~25 s after MTS-ET$^+$ application and remained stable for the remainder of the recording. An expanded view of the region indicated by the black bar shows the reduction in current occurred in a stepwise fashion (indicated by the arrows). Dashed lines indicate fully open and closed states before application of MTS-ET$^+$. Dotted lines in the expanded view indicate currents levels ascribed to the identifiable step changes in current after application of MTS-ET$^+$. The magnitude of the step change increased as modification progressed to completion. The opening events before the first identifiable step change appeared slightly diminished compared with the prereacted level (open state dashed line), indicating reactions may have taken place, but were small and not discernible as discrete steps within the open channel noise. (B) Summary of data comparing unitary conductance (left panels) and open-channel rectification of hemichannels in which positions 46 and 51 were modified to Lys, Arg, or Cys reacted with MTS-EA$^+$ or MTS-ET$^+$. wt Cx46 hemichannels are included for comparison. The solid horizontal lines denote mean values for conductance and rectification of wt Cx46 hemichannels. Error bars represent standard deviations. For each mutant, n represents the number of separate patches examined containing single hemichannels. Data for conductance and rectification were obtained from the same patches.
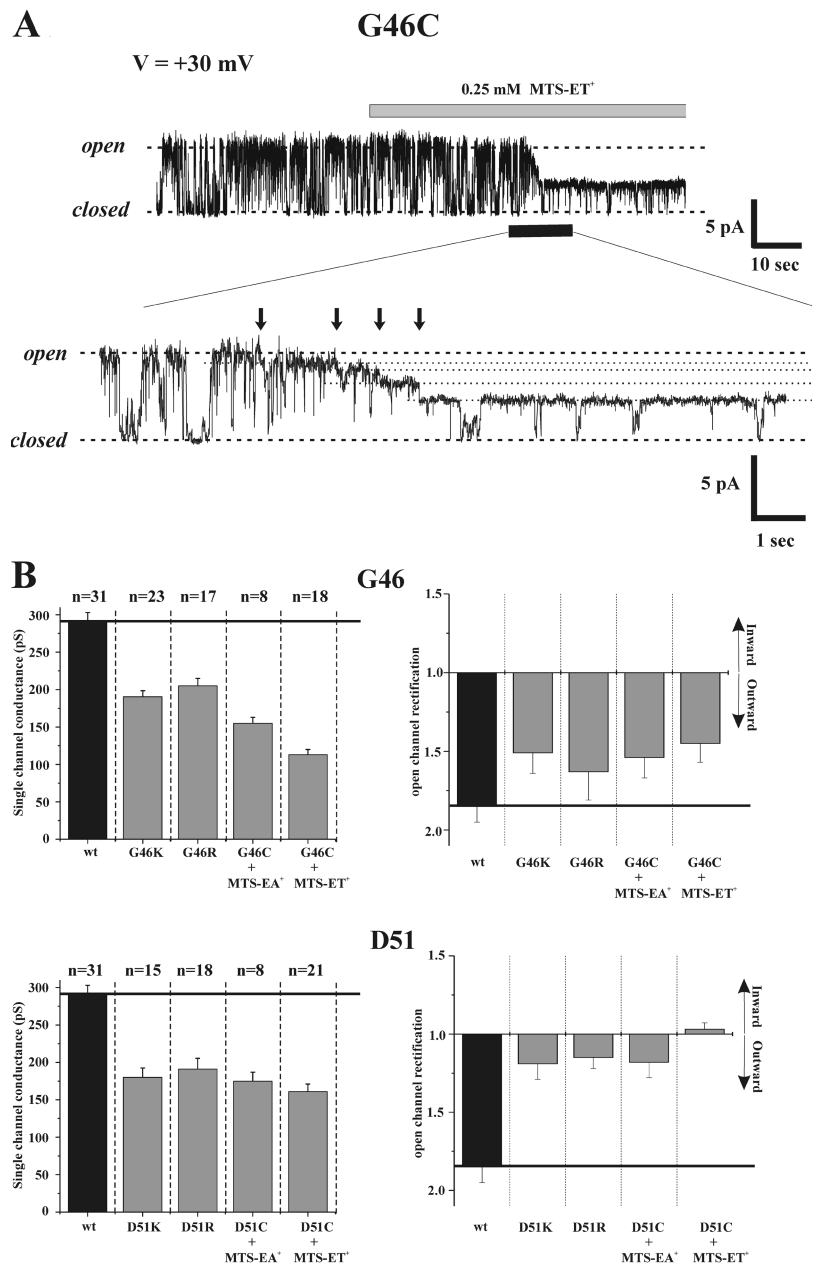
subunits. When the concentration of MTS-ET$^+$ was reduced to slow the reaction rate, multiple step changes in single hemichannel currents were resolved. Fig. 6 A shows an example of a recording from a single G46C hemichannel to which 0.25 mM MTS-ET$^+$ was applied. The dashed lines indicate the fully open and closed states of the hemichannel before application of MTS-ET$^+$. At least four step changes in current, which we provisionally ascribe to reactions with individual subunits, were evident in this example (indicated by the arrows). In five separate patches, three or four step changes were observed. An invariant pattern in all cases was that the first resolvable step reduction in conductance was the smallest and each subsequent step was in-

creasingly larger such that the last one constituted ~40% of the total reduction in conductance. A similar pattern was observed at D51C (unpublished data). The last conductance level remained stable after washout of reagent and is the same stable level achieved using a higher concentration of MTS-ET$^+$.

Although we did not observe six step changes in conductance with MTS-ET$^+$, corresponding to reactions with each of the six subunits, the final resulting conductance level observed with application of MTS-ET$^+$ was consistent among patches, stable after washout, and no additional changes in unitary conductance could be elicited upon subsequent application of MTS-ES$^-$. Also, as previously indicated, MTS-ET$^+$ had no ef-

A G46C: wt (pre-reaction)

B G46C: wt (1:1) + MST-ET$^+$

C G46C: wt (2:1) + MST-ET$^+$

D G46C + MTS-ET$^+$
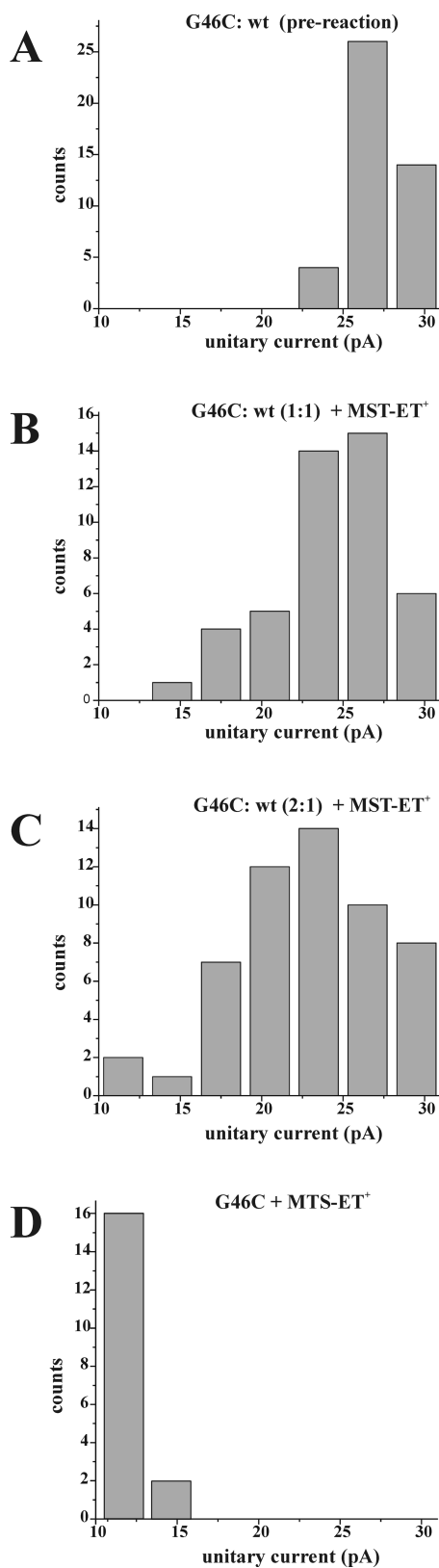
FIGURE 7. Reductions in unitary conductance of G46C hemichannels by MTS-ET$^+$ results from modification of all six subunits. In all plots, counts represent the number of hemichannels whose conductance falls within the bin width shown. All currents were

fect if oocytes were pretreated with MTS-ES$^-$. These results suggest that all subunits are modified upon application of MTS-ET$^+$ or MTS-ES$^-$, leaving none available upon subsequent MTS application.

To further test whether all six subunits are modified, we performed two additional experiments. First, we individually substituted Lys or Arg at G46 and D51 to generate mutant hemichannels in which a given residue in all six subunits was certain to be modified to a positive charge. These modifications produced hemichannels with substantially smaller unitary conductances compared with wt Cx46 (Fig. 6 B) and changes in open hemichannel current rectification correlated qualitatively with the changes observed upon MTS modification, with D51R/K showing nearly linear I-V relations and G46R/K inward rectification. Thus, properties of hemichannels in which all six subunits are modified to positive charge at a given position are similar to those in which Cys substitutions were modified by MTS-ET$^+$ or MTS-EA$^+$. Second, we coinjected oocytes with G46C and wtCx46 cRNA in 1:1 and 2:1 ratios and examined the conductances of individual hemichannels before and after treatment with MTS-ET$^+$. Subunit stoichiometries assuming equal probabilities of association have a majority of hemichannels ($\sim$80%) containing two, three, and four Cys residues with a 1:1 ratio and three, four, and five Cys residues with a 2:1 ratio. Approximately 2% and 10% of the hemichannels would be G46C homomeric for the 1:1 and 2:1 coinjection ratios, respectively. Prior to treatment with MTS-ET$^+$, single-hemichannel currents were uniform with a mean of 27.1 ± 1.7 pA at −70 mV (Fig. 7 A). After treatment, individual hemichannel currents were smaller to a variable degree. The distribution of hemichannel currents showed a shift to smaller amplitudes in the 2:1 (Fig. 7 C) compared with the 1:1 (Fig. 7 B) injection ratio. If only four Cys residues were maximally reacted in a given hemichannel, corresponding to the number of hits we maximally detect in homomeric G46C hemichannels, application of MTS-ET$^+$ to oocytes injected with the 2:1 ratio in particular, where $\sim$70% of the hemichannels would contain four or more Cys residues, should show a majority of hemichannels with cur-

measured as the chord conductance at -70 mV in symmetric IPS solution. (A) Frequency distribution of single hemichannel current amplitudes of oocytes coinjected with G46C and wtCx46 cRNAs. No differences were observed between oocytes injected with 1:1 and 2:1 ratios (G46C:wt) and the data are pooled together. (B) Frequency distribution of single-hemichannel current amplitudes of oocytes coinjected with G46C and wtCx46 cRNAs in a 1:1 ratio and treated with 1 mM MTS-ET$^+$. (C) Frequency distribution of single hemichannel current amplitudes of oocytes coinjected with G46C and wtCx46 cRNAs in a 2:1 ratio and treated with 1 mM MTS-ET$^+$. (D) Frequency distribution of single-hemichannel current amplitudes of oocytes injected only with G46C cRNA and treated with 1 mM MTS-ET$^+$.

FIGURE 8. SCAM with MT-SET$^+$ shows continued reactivity in TM1 and no evidence of reactivity in the topologically corresponding segment of TM3. Effects of Cys substitutions for TM1 residues E42 through R33 (A) and TM3 residues F175 through E166 (B). Solid horizontal lines indicate E1/TM1 and E2/TM3 borders according to Bennett et al. (1991). The change in unitary conductance represents the mean percentage change in the slope conductance compared with wt Cx46 measured at $V_m = 0$ from fitted open channel I-V relations. In general, Cys substitutions in TM1 produced increases in conductance, whereas in TM3 there was no obvious pattern. In TM1, E42C and R33C failed to form functional hemichannels and single channels were not observed from oocytes injected with V36C and I34C due to consistently low expression levels. In TM3, all Cys mutants formed functional hemichannels. Below the Cys-substitution data,

SCAM results are summarized for residues D51 through R33 (A) and residues F175 through E166 (B), which span the regions shaded in black in the corresponding illustrations of connexin subunits. In TM1, large reductions in conductance with MTS-ET$^+$ were observed at two positions, A39C and L35C. No substantial changes in conductance were observed at any position in TM3. For all mutants, the change in unitary conductance represents the mean percentage change in the slope conductance relative to the corresponding Cys substituted mutant measured at $V_m = 0$ from fitted open channel I-V relations. Data from excised patches of either configuration showed no differences and are pooled together with cell-attached recordings of prereacted oocytes. NC denotes nonfunctional hemichannels. ND denotes residues for which there was insufficient single-channel data for characterization.
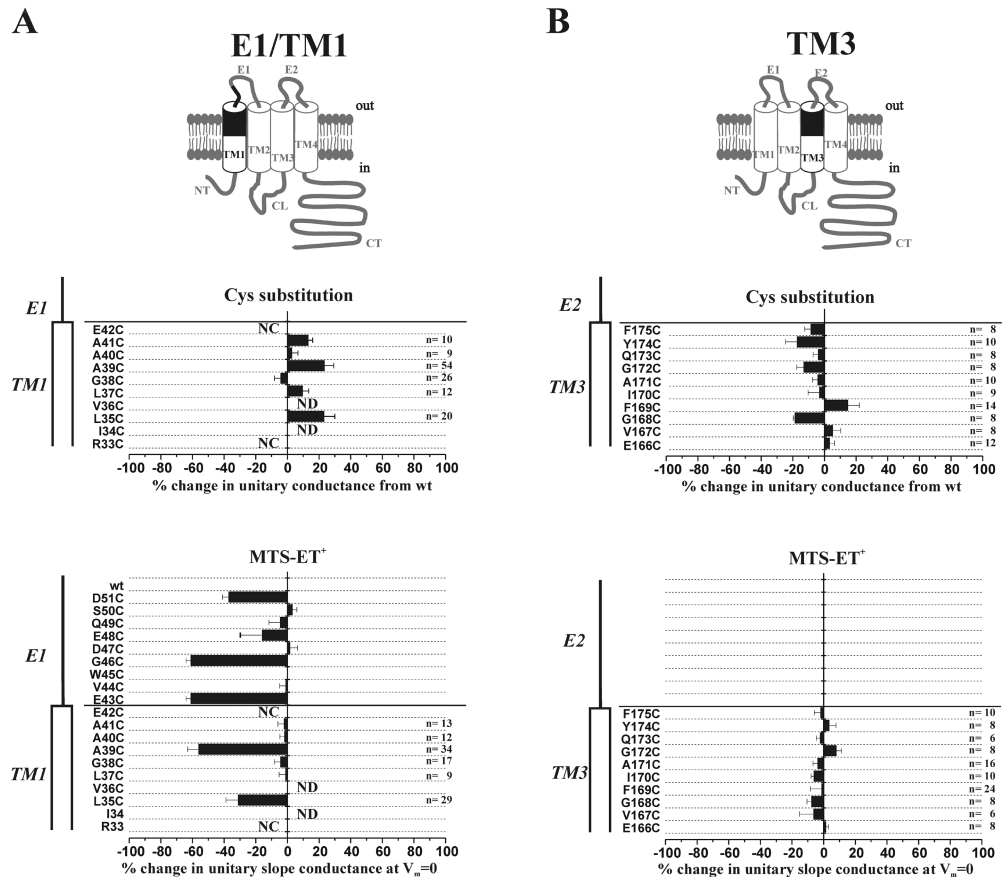
rents corresponding to the final reduced level observed in homomeric G46C hemichannels. However, the majority of hemichannels showed considerably larger conductances indicating that having four and five Cys residues available for reaction is not sufficient to produce the conductance observed in homomeric G46C hemichannels reacted with MTS-ET$^+$. Together, these results provide strong evidence that modifications with small, charged MTS reagents occur on all six subunits.

TM1 Continues as Pore-lining as the Hemichannel Enters the Transmembrane Span

Considering that E43 is pore lining, its location at the TM1/E1 border suggests that TM1 would likely continue as the pore, at least initially as the hemichannel enters into the transmembrane span. Thus, we extended our SCAM study to an additional 10 residues, E42 through R33. Thus far, only data using MTS-ET$^+$

have been obtained. Of the 10 TM1 cysteine mutants, E42C and R33C failed to induce hemichannel currents when expressed in *Xenopus* oocytes. V36C and I34C expression was often poor and never reached levels high enough to permit single-channel recordings to be obtained with regular frequency. Thus, the single-channel properties of these mutants remain uncharacterized and reactivity to MTS-ET$^+$ untested. For the other six positions, Cys substitution alone generally resulted in a slightly larger unitary conductance, particularly at two positions, A39C and L35C (Fig. 8 A). This result is in contrast to that obtained for Cys substitutions in E1, which generally produced reductions in unitary conductance. These same two residues, A39C and L35C, also displayed large (~50%) reductions in unitary conductance upon application of MTS-ET$^+$ (Fig. 8 A). The reductions in conductance were observed with hemichannels in the open state and the same results were obtained with MTS-ET$^+$ added to the extracellu-

lar or intracellular sides, thereby meeting our criteria for assignment to the pore. No effects on open hemi-channel properties were observed at A41C, A40C, G38C and L37C with MTS-ET$^+$ concentrations as high as 1 mM. Based on these data, we conclude that TM1 continues from E1 as a pore-lining domain in Cx46 hemichannels in the region predicted to enter the transmembrane span from the extracellular side.

Given that TM3 has been reported to be pore lining in Cx32 cell–cell channels (Skerrett et al., 2002), we also tested MTS-ET$^+$ accessibility of 10 residues within the extracellular portion of TM3 from F175 to E166, a region that starts at the TM3/E2 border and corresponds topologically to the tested region in TM1. All 10 TM3 Cys-substituted mutants formed functional hemichannels and displayed small increases or decreases in unitary conductance compared with wt Cx46. However, none of the mutants showed any appreciable change in open-hemichannel properties upon application of MTS-ET$^+$ (Fig. 8 B).

DISCUSSION

The utility of probing solvent-accessible domains of proteins using SCAM is exemplified by its widespread use and the corroboration of findings using SCAM with other biophysical methodologies. For ion channels, SCAM has been applied to identify aqueous-accessible domains, most notably those that line the channel pore, as well as to obtain additional information about channel structure such as locations of gates and voltage sensors, sites of channel blockers and regions of ligand binding (see Karlin, 2001; Bera et al., 2002). The permanently charged MTS reagents, MTS-ET$^+$ and MTS-ES$^-$, have been most widely used and their accessibility on a rapid time scale is generally accepted as confined to residues on hydrophilic surfaces (Karlin and Akabas, 1998). A caveat is that hydrophilic surfaces found deep within the transmembrane span of ion channels may represent aqueous crevices, remote from the pore, connected to extracellular or intracellular compartments. However, the pore in an open channel is unique in that it is a hydrophilic surface confluent with the aqueous compartments on both sides. We reasoned that in large channels, such as those formed by connexins, residues would be readily accessible to MTS reagents along the entire length of the pore and reactivity from either side of the membrane would raise confidence in assignment to the pore. Although it is possible that residues not in the pore can be accessible from either side by translocation back and forth across the membrane, as demonstrated for colicin and diphtheria toxin channels (Slatin et al., 1994; Senzel et al., 2000), such translocations represent large conformational changes and can be distinguished by state dependence of accessibility. Thus, our criterion for assignment to the pore included accessibility from either side with the channel being open. This does not exclude reactivity occurring in the closed state from one or the other side.

Satisfying these criteria required that reactions be monitored in single channels with either side of the channel accessible to perfusion. We could readily satisfy these criteria by using unapposed connexin hemichannels that function in the plasma membranes of isolated cells. Hemichannels allow use of conventional patch clamp techniques to stably record single channels and also to gain ready access to either side by means of excised inside-out and outside-out patch configurations (Trexler et al., 1996, 1999). Cx46 hemichannels have a large unitary conductance and a high open probability in low extracellular Ca^{2+} over a wide voltage range that provided good resolution of effects of modification on single channels. Macroscopic and single-channel studies indicate that hemichannel structure is minimally different from that of the cell–cell channel so that SCAM studies on hemichannels should apply to cell–cell channels as well. There is strong correspondence between voltage and chemical gating in hemichannels and cell–cell channels suggesting conservation of structure mediating these processes (Ebihara et al., 1995; Trexler et al., 1996, 1999; Oh et al., 2000; Beahm and Hall, 2002). Conservation of pore structure is indicated by conductance and selectivity studies that compare hemichannels and cell–cell channels composed of the same connexin isoforms (Trexler et al., 2000; Valiunas and Weingart, 2000). Furthermore, structural similarity is suggested by correspondence of the effects CMTX mutations on function of Cx32 hemichannels and cell–cell channels (Castro et al., 1999). Some qualitative differences in dye selectivity between undocked hemichannels versus cell–cell channels have been inferred from comparisons of rates of dye uptake in single cells expressing connexins and intercellular transfer in the same cells when paired (Valiunas, 2002). Although some structural rearrangement is certain to occur upon docking of unapposed hemichannels, it is unlikely that hemichannels and cell–cell channels with correlative gating, conductance, and permeability characteristics represent substantially different structural configurations.

Effects of MTS Modification on Cx46 Hemichannels Are Predominantly Electrostatic Consistent with a Large, Aqueous Pore Dominated by Fixed Negative Charge

At each of the residues in E1 and TM1 that met our criteria for assignment to the pore, modification to a positive charge with MTS-ET$^+$ resulted in a large decrease in unitary conductance. For the E1 residues, which we studied more extensively, similarly large reductions in conductance were produced by modification with MTS-EA$^+$, as well as by mutation to Arg or Lys. Conversely,
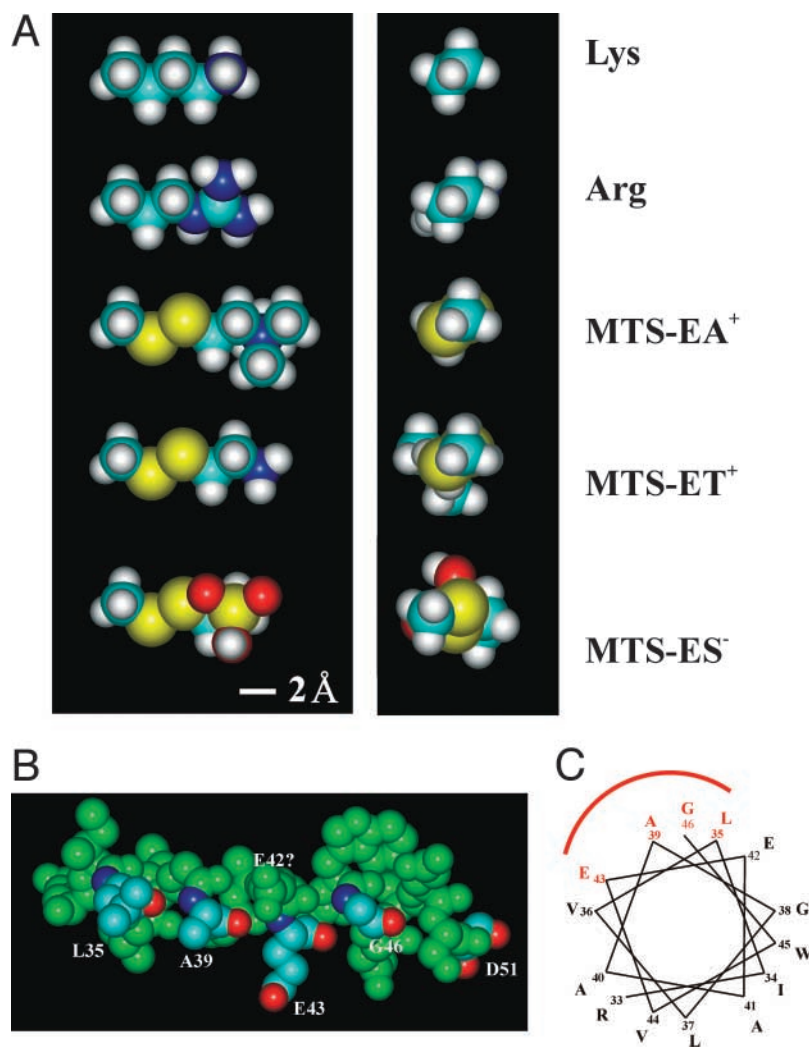
FIGURE 9. Reactivity between L35 and G46 follows an α-helical pattern. (A) Space-fill models comparing side chains of residues composed of Lys, Arg, and Cys modified by MTS-EA$^+$, MTS-ET$^+$, and MTS-ES$^-$. The color code for atoms is H (white), C (cyan), N (blue), O (red), and S (yellow). Left and right panels show views along and down the long-axes of the side chains, respectively. (B) Space-fill α-helical representation of residues R33 through D51 of Cx46. Residues assigned to the pore are shown in color. All other residues are in green. With the exception of D51C, reacted residues fall along one face of the helix suggesting a departure from an α-helical transmembrane secondary structure in the E1/TM1 border region. (C) Helical wheel representation of residues R33 through G46 of Cx46. Reacted residues (red) reside on one side subtending an arc of ~80 degrees. For A and B the models were generated using Hyperchem, release 3 (Hypercube, Inc.).

modification with MTS-ES$^-$ either had little effect or modestly increased conductance. Qualitatively, these data are consistent with a charge profile in the wt Cx46 hemichannel dominated by fixed negative charges, as previously suggested (Trexler et al., 2000), that results in a predominance of cations in the pore. Introduction of a positive charge in the pore would tend to reduce the cation concentration, thereby substantially reducing conductance. Maintenance of negative charge or addition of negative charge, particularly in a region of the pore already containing a high negative charge density could conceivably have little effect.

Comparing the effects of MTS modifications and substitutions indicates that side-chain electrostatics rather than volume is most influential in producing the observed effects on open channel properties. Modification to positive charge, whether by MTS-ET$^+$, MTS-EA$^+$, or Arg/Lys substitution all produced substantial reductions in unitary conductance. Modification to negative charge by MTS-ES$^-$ produced either no decrease or even an increase in unitary conductance,

even though the sulphonate head of this reagent is similar in bulk to the trimethylammonium head of MTS-ET$^+$. At D51C and G46C, we did observe that modification with MTS-ET$^+$ reduced conductance and inward rectification slightly more than the smaller MTS-EA$^+$ (Fig. 5). Also modification with either positively charged reagent reduced conductance more than substitution with Arg or Lys. Space-fill models show that side chains of Cys residues modified by MTS-ET$^+$ and MTS-EA$^+$ are bulkier than those of Arg or Lys (Fig. 9 A). Thus, it appears that the modest differences in open-channel properties among hemichannels containing positively charged side chains correlates with side-chain volume, suggesting that size as well as charge density within the pore may differ sufficiently in the various modified or substituted configurations to produce small, but measurable effects. These differences were more pronounced at G46 and E43 (unpublished data) than D51 suggesting, perhaps, that the pore narrows near the TM1/E1 border and widens again as the pore extends into the extracellular gap. This gross mo-

lecular profile of narrowing at the extracellular membrane border and widening in the extracellular gap is consistent with that reported for the Cx43 GJ channel structure reported by (Unger et al., 1999). We did not examine substitutions with residues containing large, branched side chains that may cause reductions in conductance due to steric considerations.

At each of the accessible positions, the rapidity with which we observed MTS reactions, as well as the small effects caused by MTS-ES$^-$ modification are consistent with the Cys residues being largely ionized. MTS reagents react $\sim10^9$ times faster with the ionized compared with the unionized thiol (Karlin and Akabas, 1998). At E43, Cys substitution had no measurable effect, suggesting Cys at this position maintains complete ionization and bears an equivalent charge to the naturally occurring Glu. At D51, Cys substitution resulted in a modest decrease in conductance and rectification suggesting that Cys at position 51 has less effective charge than the naturally occurring Asp and may signify that there is incomplete ionization and/or reduced charge density because of smaller side-chain volume. Consistent with these possibilities is a modest increase in conductance, even beyond wt Cx46, upon modification with MTS-ES$^-$; the latter should be fully ionized at neutral pH and has a larger side-chain volume that could increase local charge density in the pore compared with Asp. More difficult to explain is the lack of a measurable effect of Cys substitution at G46. Even a partially ionized Cys should introduce more charge than Gly, barring exposed backbone charges. It is possible that with flanking negative charges at E43 and D51, there is such a high local charge density, and hence local concentration of cation, that additional negative charge at G46 would have a negligible effect. At A39 and L35, farther from the region of high negative charge density, Cys substitutions alone increased unitary conductance (Fig. 8 A). These results can be explained by a local increase in cation concentration at these locations, and hence increased conductance, as a result of replacement of uncharged side chains with negatively charged Cys side chains. The effects of modification with MTS-ES$^-$ at A39 and L35 were not examined. Also, we did not examine effects of altered pH on any of the Cys-substituted hemichannel currents.

Positional Effect of Cys Substitutions and MTS Modifications on Open Hemichannel Properties Provides a Relative Physical Mapping of Residues onto the Pore

Accepted connexin topology places E43 close to the TM1/E1 border, $\sim1/3$ the distance from the extracellular end of an unapposed hemichannel. Extension into E1 should place G46 and D51 extracellular to E43, with D51 likely the farthest extracellular residue

we examined. Similarly, extension into TM1 should place A39 cytoplasmic to E43 followed by L35. This arrangement, which follows the basic topology of connexins, is supported by the qualitative differences in the effects caused by the Cys substitutions alone and their modification with MTS reagents. Given that a rectifying open-channel I-V relation is caused by an asymmetric charge profile within the channel pore, charges located toward the ends create the largest asymmetries. Of all the positions that met our criteria for assignment to the pore, modification at D51 had the largest impact on open-channel rectification. A nearly 2:1 inward rectification at ±70 mV was converted to slightly outward rectification with MTS-ET$^+$ modification. G46C, E43C, A39C, and L35C all retained inward rectification when modified by MTS-ET$^+$. Thus, conversion of D51 to a positive charge, by itself, can abolish inward rectification and maintenance of negative charge at this position, even with any of the other positions modified to positive charge, is sufficient to maintain inward rectification. These results are consistent with D51 contributing charge near the extracellular end of the pore. As previously indicated, Cys substitutions alone at A39 and L35 could provide negative charge through ionization. The modestly reduced inward rectification characteristic of these substitutions (unpublished data) is qualitatively consistent with positions further along the pore away from the extracellular end. Overall, the pattern of reactivity from L35 through G46 follows along one side of an α-helix (Fig. 9, B and C). E42 also appears that it could be accessible, but the E42C mutation did not form viable hemichannels. If E42 were in the pore, it is surprising that a Cys substitution would cause loss of function and implies that E42 may have a functional interaction with another residue. The overall α-helix pattern appears disrupted at D51. The E1 and E2 loops have been proposed to adopt an antiparallel β-sheet conformation (Foote et al., 1998). Perhaps the initial segment of E1 is a transitional region between the α-helical TM1 domain and the β-sheet E1 domain.

We showed previously that substitution of the E1 domain of Cx46 with Cx32 sequence, which includes a D51S substitution, created a hemichannel with substantial outward rectification and loss of a preference for cations (Trexler et al., 2000). In this chimera, E43 is changed to Ser, but does not obviously explain the outward rectification. The Q49K substitution that occurs in the chimera could produce outward rectification by introduction of positive charge at the extracellular end, but we did not see evidence of accessibility of Q49C by MTS reagents. It is possible that a positive charge at this position, due to close proximity to the pore, when combined with other charge changes in E1 may be sufficient to produce outward rectification.

FIGURE 10. Schematic of an idealized single-channel current showing the proposed pattern of subunit modification that occurs with MTS-ET$^+$. The lower dashed line indicates the fully closed state (closed) and the upper dashed line the open state before application of MTS-ET$^+$ (open). We envision six step changes in conductance (indicated by the numbers) in the pattern shown, each representing a reaction at an individual subunit. The subunit reactions become progressively larger such that the first one is small and the last one constitutes nearly 40% of the total conductance change. The latter subunit modifications are large enough to be observed as discrete step changes in current, whereas the initial modifications are likely obscured by the open channel noise.
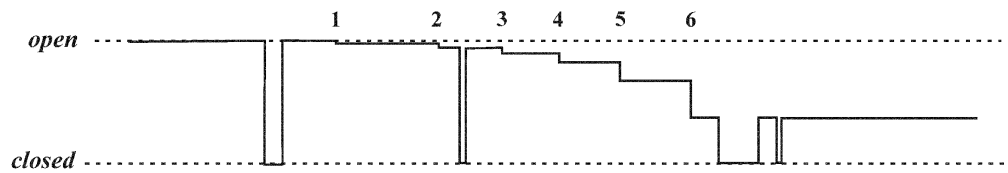
Evidence of a Large Pore with All Six Subunits Accessible to Modification

Several experimental lines of evidence suggest all six subunits of the Cx hemichannel, at least in the E1 domain, are modified in a single channel. First, D51C, G46C, or E43C hemichannels modified by any one of the MTS derivatives were refractory to subsequent modification, suggesting all available sites were occupied during the first application. Second, the effects of modification by MTS-ET$^+$ and MTS-EA$^+$ were similar to substitution with Arg or Lys, where all subunits at a given position carry a positive charge. Finally, application of MTS-ET$^+$ to oocytes coinjected with G46C and wtCx46 cRNA in ratios that should produce a substantial fraction of heteromeric hemichannels containing four or more G46C residues, rarely reduced single channel currents to levels observed in homomeric G46C hemichannels. Shifts in the distribution of hemichannel conductances in 1:1 compared with 2:1 injection ratios indicated that heteromeric hemichannels containing mutant and wt subunits were indeed formed.

Although multiple step changes, usually three or four ascribed to modifications, were resolvable in recordings containing single D51C or G46C hemichannels, we did not observe six step changes corresponding to reactions at each of the subunits. However, before the first resolvable step change in conductance, single-channel current often appeared slightly diminished compared with that before MTS application. We ascribe the slight reduction in conductance to modifications of one or two subunits that produce small reductions in current not resolvable as discrete step changes amidst the large open channel noise. This possibility is plausible given the pattern of conductance change we observed in single hemichannels, i.e., the step reductions were progressively larger such that the last step change constituted nearly 40% of the total conductance change. Thus, the first two or three modifications may indeed have caused small conductance changes buried in the open-channel noise, resulting in a pattern such as that illustrated in Fig. 10. This interpreta-

tion is also consistent with the results obtained from the 1:1 coinjection experiments showing a majority of hemichannels with modestly smaller conductances after application of MT-SET$^+$, even though $\sim$66% of the hemichannels should contain three or more subunits possessing a substituted Cys residue.

As subunits are being modified in a single hemichannel, there are a number of possible combinations of modified and unmodified subunits, yet the same overall pattern of conductance change was consistently observed. This result suggests that either there is a preferential pattern of modification in a single hemichannel or that the relevant electrostatic property at a given position along the pore is the combined net charge contributed by the subunits, regardless of the pattern by which that net charge is achieved. Each increasingly larger step change with each positive charge modification could result from the creation of an increasingly stronger dipole in a pore that is dominated by fixed negative charge. If so, modifications that add more negative charge would not show the same pattern of conductance changes. Unfortunately, the change in conductance with MTS-ES$^-$ was only observed at D51C and was too small to allow distinction of individual subunit reactions.

SCAM Studies in Cx46 and Cx32

The first SCAM study aimed at identifying connexin pore-lining domains used hemichannels and maleimido-butyryl-biocytin, MBB, as the thiol reagent (Zhou et al., 1997). Accessibility was reported in TM1 at positions I34 and L35 in Cx46 hemichannels and the equivalent positions I33 and M34 in the chimeric Cx32*43E1 hemichannel. Accessibility to TM3 in the same study was inconclusive. Additional support for TM1 as pore-lining was that replacement of TM1 in Cx32*43E1 chimeric hemichannels with Cx46 sequence changed unitary conductance to that of wt Cx46 hemichannels, interpreted as resulting from an exchange of permeation pathways (Hu and Dahl, 1999). That TM1 might contribute to the pore was also suggested from biophysical characterization of a missense mutation in TM1, S26L, which causes CMTX (Oh et al., 1997). This mutation

appeared to reduce the effective pore radius of Cx32 from ~7 Å to <3 Å, consistent with a constriction introduced by replacement of Ser with the more bulky Leu residue. Recently, Skerrett et al. (2002), using a cut-open oocyte preparation to SCAM cell–cell channels and also using MBB as the thiol reagent, reported TM3 as the major pore-lining helix in Cx32 cell–cell channels. Seven residues, spanning from Y135 to Y151, were reported to be reactive, as well as residues in TM1 and TM2, which were proposed to contribute to the cytoplasmic end of the pore with the channel in closed and open states, respectively.

Our assignment of TM1 to the pore in the region where the channel extends into the transmembrane span from the extracellular side differs from that of Skerrett et al. (2002), who reported TM3 to be pore lining throughout much of the transmembrane span. We observed no effects of MTS-ET[+] application to TM3 residues V167C, F169C, and A171C in Cx46, which correspond to the reported accessible sites A147, F149, and Y151, respectively, in Cx32. Although we did not observe an effect of MTS-ET[+] in TM3, we cannot rule out silent reactions without further testing with larger reagents and charge substitutions. Close helical packing together with the large size of the pore could conceivably allow for two TM domains to contribute to the pore in the same topological region. Also, we cannot say that TM1 contributes to the pore throughout the entire TM span as reactivity has not been confirmed for residues beyond L35.

Our results are consistent with the conclusions of Zhou et al. (1997) using SCAM with MBB and of Hu and Dahl (1999) using domain substitution that TM1 contributes to the pore. Although Hu and Dahl (1999) reported correspondence between single channel conductance and substitution of the TM1 domain of Cx46 into Cx32*43E1, we have shown that a number of chimeric hemichannels formed of Cx32 and Cx46 that have TM1 of Cx46 in common can vary fivefold in single channel conductance (Trexler et al., 2000). Also, as we have shown here, E1 contributes to the pore and contains charged residues that differ between Cx32 and Cx46 and that significantly affect single-channel conductance and open-channel rectification. Thus, differences in TM1 between Cx46 and Cx32*43E1 could be largely responsible for the conductance difference between those two hemichannels in particular, but pore-lining residues outside the putative TM span of Cx channels can clearly contribute significantly to single-channel conductance. Cx channels constitute large pores and are not likely to have distinct regions, like the selectivity filters of a K^{+}, Na^{+}, or Ca^{2+} channels that determine conductance and selectivity.

Our SCAM study differs from that of Zhou et al. (1997) and Skerrett et al. (2002) in two basic ways, the thiol reagents used and reliance on single-channel rather than macroscopic data. Monitoring single channels allowed clear separation of effects of gating from those directly relevant to ion transport through open channels, namely unitary conductance and open-channel rectification. The thiosulphonates we used, MTS-EA[+], MTS-ET[+], and MTS-ES[−], are relatively small and highly specific for sulfhydryls. Each would fit in a cylinder ~6 Å in diameter (Karlin and Akabas, 1998; Bera et al., 2002) and is well within the permeable size range of Cx channels; the latter was corroborated by our demonstrated reactivity from either side of the membrane. Reactions with these MTS reagents occur quickly with the ionized form, S[−], and the rapidity (seconds) with which we observed reactions argues in favor of residues on readily-accessible water surfaces. Given enough time, Cys residues buried within a protein can also be modified (Karlin and Akabas, 1998). Maleimides react with amines at pH above 7.5 raising the possibility of nonspecificity and the reported time course over which conductance changes took place in Cx32 cell–cell channels was slow, tens of minutes (Skerrett et al., 2002), raising the possibility of access to some residues in the protein interior. MBB is large and closer to the size limit of permeation so that if it did react within the pore, its presence would likely produce a large reduction in conductance, if not complete block, upon modification. At one position, L35C, MBB accessibility was examined at the single hemichannel level and showed a large reduction in conductance of ~80% (Pfahnl and Dahl, 1998). This reduction was considerably greater than that observed macroscopically (~50%). In general, the reported reductions in macroscopic currents with MBB are relatively small in Cx32 cell–cell channels, ranging from ~10–30%, and modest, ~40–50%, in Cx46 and Cx32*Cx43E1 hemichannels (Zhou et al., 1997; Skerrett et al., 2002). It is possible that steric restrictions limit reactivity of MBB to fewer or even single subunits, a possibility supported by the observation of only a single-step change in conductance at L35C (Pfahnl and Dahl, 1998). Steric restrictions coupled with altered gating that increases open probability could result in smaller than expected reductions in macroscopic currents.

We do not expect that the different accessibility patterns assigned to Cx46 and Cx32 result from differences between hemichannels and cell–cell channels nor to the fact that connexins are categorized into two major groups based on sequence homology, with Cx32 belonging to Group I (β) and Cx46 to Group II (α). As previously indicated, both hemichannel and cell–cell channel configurations share many functional features indicative of conserved structure. Also, while there may be some differences in structural features between channels formed of Group I and II connexins, the

same residues were found accessible to MBB in Cx46 and Cx32*43E1 hemichannels (Zhou et al., 1997); the latter is a chimera in which only E1 differs on a Cx32 background and has been shown to have properties similar to Cx32 cell–cell channels (Oh et al., 1999, 2000). Nonetheless, a systematic comparison of accessibility in Cx46 and Cx32 hemichannels and cell–cell channels using the same thiol reagents would help resolve these issues.

In summary, we demonstrate a substantial pattern of reactivity to MTS reagents over a stretch of 17 amino acids, D51 through L35. Our data provide evidence of a large pore with the side chains of residues at equivalent positions on each subunit accessible to MTS modification. The valence of the side chain strongly influences single-channel conductance and the shape of the current-voltage relation of single open hemichannels. Two of the accessible residues in E1, E43 and D51, are negatively charged and likely comprise the locus of fixed negative charge in Cx46 previously indicated by domain substitution. Mutational studies have shown the second extracellular loop, E2, to be involved in connexin compatibility, i.e., their ability to dock (White et al., 1994). It may be that the continuous inner and outer walls of protein demonstrated in structural models of Cx43 channels (Unger et al., 1999) are predominantly comprised of the E1 and E2 domains, respectively.

REFERENCES

Beahm, D.L., and J.E. Hall. 2002. Hemichannel and junctional properties of connexin 50. *Biophys. J.* 82:2016–2031.

Bennett, M.V., L.C. Barrio, T.A. Bargiello, D.C. Spray, E. Hertzberg, and J.C. Saez. 1991. Gap junctions: new tools, new answers, new questions. *Neuron.* 6:305–320.

Bera, A.K., M. Chatav, and M.H. Akabas. 2002. GABA(A) receptor M2-M3 loop secondary structure and changes in accessibility during channel gating. *J. Biol. Chem.* 277:43002–43010.

Bergoffen, J., S.S. Scherer, S. Wang, M.O. Scott, L.J. Bone, D.L. Paul, K. Chen, M.W. Lensch, P.F. Chance, and K.H. Fischbeck. 1993. Connexin mutations in X-linked Charcot-Marie-Tooth disease. *Science.* 262:2039–2042.

Castro, C., J.M. Gomez-Hernandez, K. Silander, and L.C. Barrio. 1999. Altered formation of hemichannels and gap junction channels caused by C-terminal connexin-32 mutations. *J. Neurosci.* 19:3752–3760.

Cha, A., and F. Bezanilla. 1998. Structural implications of fluorescence quenching in the Shaker K+ channel. *J. Gen. Physiol.* 112:391–408.

Dahl, G., E. Levine, C. Rabadan Diehl, and R. Werner. 1991. Cell/cell channel formation involves disulfide exchange. *Eur. J. Biochem.* 197:141–144.

Ebihara, L., V.M. Berthoud, and E.C. Beyer. 1995. Distinct behavior of connexin56 and connexin46 gap junctional channels can be predicted from the behavior of their hemi-gap- junctional channels. *Biophys. J.* 68:1796–1803.

Ebihara, L., and E. Steiner. 1993. Properties of a nonjunctional current expressed from a rat connexin46 cDNA in Xenopus oocytes. *J. Gen. Physiol.* 102:59–74.

Foote, C.I., L. Zhou, X. Zhu, and B.J. Nicholson. 1998. The pattern of disulfide linkages in the extracellular loop regions of connexin 32 suggests a model for the docking interface of gap junctions. *J. Cell Biol.* 140:1187–1197.

Glauner, K.S., L.M. Mannuzzu, C.S. Gandhi, and E.Y. Isacoff. 1999. Spectroscopic mapping of voltage sensor movement in the Shaker potassium channel. *Nature.* 402:813–817.

Harris, A.L. 2001. Emerging issues of connexin channels: biophysics fills the gap. *Q. Rev. Biophys.* 34:325–472.

Hertzberg, E.L., R.M. Disher, A.A. Tiller, Y. Zhou, and R.G. Cook. 1988. Topology of the Mr 27,000 liver gap junction protein. Cytoplasmic localization of amino- and carboxyl termini and a hydrophilic domain which is protease-hypersensitive. *J. Biol. Chem.* 263:19105–19111.

Hu, X., and G. Dahl. 1999. Exchange of conductance and gating properties between gap junction hemichannels. *FEBS Lett.* 451:113–117.

Ionasescu, V., C. Searby, and R. Ionasescu. 1994. Point mutations of the connexin32 (GJB1) gene in X-linked dominant Charcot-Marie-Tooth neuropathy. *Hum. Mol. Genet.* 3:355–358.

Karlin, A. 2001. Scam feels the pinch. *J. Gen. Physiol.* 117:235–238.

Karlin, A., and M.H. Akabas. 1998. Substituted-cysteine accessibility method. *Methods Enzymol.* 293:123–145.

Kelsell, D.P., J. Dunlop, H.P. Stevens, N.J. Lench, J.N. Liang, G. Parry, R.F. Mueller, and I.M. Leigh. 1997. Connexin 26 mutations in hereditary non-syndromic sensorineural deafness. *Nature.* 387:80–83.

Mackay, D., A. Ionides, Z. Kibar, G. Rouleau, V. Berry, A. Moore, A. Shiels, and S. Bhattacharya. 1999. Connexin46 mutations in autosomal dominant congenital cataract. *Am. J. Hum. Genet.* 64:1357–1364.

Oh, S., C.K. Abrams, V.K. Verselis, and T.A. Bargiello. 2000. Stoichiometry of transjunctional voltage-gating polarity reversal by a negative charge substitution in the amino terminus of a connexin32 chimera. *J. Gen. Physiol.* 116:13–31.

Oh, S., Y. Ri, M.V. Bennett, E.B. Trexler, V.K. Verselis, and T.A. Bargiello. 1997. Changes in permeability caused by connexin 32 mutations underlie X-linked Charcot-Marie-Tooth disease. *Neuron.* 19:927–938.

Oh, S., J.B. Rubin, M.V. Bennett, V.K. Verselis, and T.A. Bargiello. 1999. Molecular determinants of electrical rectification of single channel conductance in gap junctions formed by connexins 26 and 32. *J. Gen. Physiol.* 114:339–364.

Paul, D.L. 1986. Molecular cloning of cDNA for rat liver gap junction protein. 1986. *J. Cell Biol.* 103:123–134.

Paul, D.L., L. Ebihara, L.J. Takemoto, K.I. Swenson, and D.A. Goodenough. 1991. Connexin46, a novel lens gap junction protein, induces voltage-gated currents in nonjunctional plasma membrane of Xenopus oocytes. *J. Cell Biol.* 115:1077–1089.

Pfahnl, A., and G. Dahl. 1998. Localization of a voltage gate in connexin46 gap junciton hemichannels. *Biophys. J.* 75:2323–2331.

Richard, G., L.E. Smith, R.A. Bailey, P. Itin, D. Hohl, E.H. Epstein, Jr., J.J. DiGiovanna, J.G. Compton, and S.J. Bale. 1998. Mutations in the human connexin gene GJB3 cause erythrokeratodermia

variabilis. *Nat. Genet.* 20:366–369.

Rubin, J.B., V.K. Verselis, M.V. Bennett, and T.A. Bargiello. 1992a. A domain substitution procedure and its use to analyze voltage dependence of homotypic gap junctions formed by connexins 26 and 32. *Proc. Natl. Acad. Sci. USA.* 89:3820–3824.

Rubin, J.B., V.K. Verselis, M.V. Bennett, and T.A. Bargiello. 1992b. Molecular analysis of voltage dependence of heterotypic gap junctions formed by connexins 26 and 32. *Biophys. J.* 62:183–193.

Senzel, L., M. Gordon, R.O. Blaustein, K.J. Oh, R.J. Collier, and A. Finkelstein. 2000. Topography of diphtheria Toxin's T domain in the open channel state. *J. Gen. Physiol.* 115:421–434.

Shiels, A., D. Mackay, A. Ionides, V. Berry, A. Moore, and S. Bhattacharya. 1998. A missense mutation in the human connexin50 gene (GJA8) underlies autosomal dominant "zonular pulverulent" cataract, on chromosome 1q. *Am. J. Hum. Genet.* 62:526–532.

Skerrett, I.M., J. Aronowitz, J.H. Shin, G. Cymes, E. Kasperek, F.L. Cao, and B.J. Nicholson. 2002. Identification of amino acid residues lining the pore of a gap junction channel. *J. Cell Biol.* 159:349–360.

Slatin, S.L., X.Q. Qiu, K.S. Jakes, and A. Finkelstein. 1994. Identification of a translocated protein segment in a voltage-dependent channel. *Nature.* 371:158–161.

Trexler, E.B., M.V. Bennett, T.A. Bargiello, and V.K. Verselis. 1996. Voltage gating and permeation in a gap junction hemichannel. *Proc. Natl. Acad. Sci. USA.* 93:5836–5841.

Trexler, E.B., F.F. Bukauskas, M.V. Bennett, T.A. Bargiello, and V.K. Verselis. 1999. Rapid and direct effects of pH on connexins revealed by the connexin46 hemichannel preparation. *J. Gen. Physiol.* 113:721–742.

Trexler, E.B., F.F. Bukauskas, J. Kronengold, T.A. Bargiello, and V.K. Verselis. 2000. The first extracellular loop domain is a major determinant of charge selectivity in connexin46 channels. *Biophys. J.* 79:3036–3051.

Unger, V.M., N.M. Kumar, N.B. Gilula, and M. Yeager. 1999. Three-dimensional structure of a recombinant gap junction membrane channel. *Science.* 283:1176–1180.

Valiunas, V. 2002. Biophysical properties of connexin-45 gap junction hemichannels studied in vertebrate cells. *J. Gen. Physiol.* 119:147–164.

Valiunas, V., E.C. Beyer, and P.R. Brink. 2002. Cardiac gap junction channels show quantitative differences in selectivity. *Circ. Res.* 91:104–111.

Valiunas, V., and R. Weingart. 2000. Electrical properties of gap junction hemichannels identified in transfected HeLa cells. *Pflugers Arch.* 440:366–379.

Veenstra, R.D., H.Z. Wang, D.A. Beblo, M.G. Chilton, A.L. Harris, E.C. Beyer, and P.R. Brink. 1995. Selectivity of connexin-specific gap junctions does not correlate with channel conductance. *Circ. Res.* 77:1156–1165.

Verselis, V.K., and F.F. Bukauskas. 2002. Connexin-GFPs shed light on regulation of cell–cell communication by gap junctions. *Curr. Drug Targets.* 3:483–499.

Verselis, V.K., E.B. Trexler, and F.F. Bukauskas. 2000. Connexin hemichannels and cell–cell channels: comparison of properties. *Braz. J. Med. Biol. Res.* 33:379–389.

White, T.W., R. Bruzzone, S. Wolfram, D.L. Paul, and D.A. Goodenough. 1994. Selective interactions among the multiple connexin proteins expressed in the vertebrate lens: the second extracellular domain is a determinant of compatibility between connexins. *J. Cell Biol.* 125:879–892.

Willecke, K., J. Eiberger, J. Degen, D. Eckardt, A. Romualdi, M. Guldenagel, U. Deutsch, and G. Sohl. 2002. Structural and functional diversity of connexin genes in the mouse and human genome. *Biol. Chem.* 383:725–737.

Zhou, X.W., A. Pfahnl, R. Werner, A. Hudder, A. Llanes, A. Luebke, and G. Dahl. 1997. Identification of a pore lining segment in gap junction hemichannels. *Biophys. J.* 72:1946–1953.